

FIG. 8. The cross-section factor  $S(E)$  as a function of the center-of-mass energy. The bars and solid curve are again the experimental values and the prediction of Ref. 4, respectively. At the intercept,  $S_0 = 0.47 \pm 0.05$  keV-b, and  $(dS/dE)_0 = -2.8 \times 10^{-4}$  b.

which are considerably more accurate than our lowest energy points.

There may be some question as to whether the normalization for extrapolation purposes should not have been made to just the low-energy measurements. If such a normalization is made using only the data for

$E_{c.m.} \leq 625$  keV, one obtains an intercept of  $S_0 = 0.51 \pm 0.07$  keV-b.

A combination of the  $S$ -factor intercepts of the other proton-proton-chain reactions with this new value for the  $\text{He}^3(\alpha, \gamma)\text{Be}^7$  reaction allows us to determine the importance of each of the  $\text{He}^3$ -burning reactions as terminations for the proton-proton chain. A detailed discussion of the termination of this chain will be published elsewhere<sup>14</sup>; it is sufficient to note here that the new intercept is appreciably smaller than the value of 1.2 keV-b previously published by Holmgren and Johnston,<sup>7</sup> and consequently that in the temperature range below  $16 \times 10^6$  K this new value reduces the importance ascribed in Refs. 5 and 6 to  $\text{He}^3(\alpha, \gamma)\text{Be}^7$  as a  $\text{He}^3$ -burning reaction in stars like the sun.

#### ACKNOWLEDGMENTS

We are happy to acknowledge the assistance of the staff of the Kellogg Radiation Laboratory in carrying out this experiment. In particular, we are grateful to Professor William A. Fowler and Dr. T. A. Tombrello for their stimulus and helpful discussions.

<sup>14</sup> P. D. Parker, J. N. Bahcall, and W. A. Fowler, *Astrophys. J.* (to be published).

## Direct-Capture Model for the $\text{He}^3(\alpha, \gamma)\text{Be}^7$ and $\text{T}(\alpha, \gamma)\text{Li}^7$ Reactions\*

T. A. TOMBRELLO† AND P. D. PARKER

*California Institute of Technology, Pasadena, California*

(Received 8 May 1963)

Using the  $\text{He}^3 + \text{He}^4$  scattering phase shifts, the cross section for the  $\text{He}^3(\alpha, \gamma)\text{Be}^7$  reaction is calculated on the basis of a  $\text{He}^3 + \text{He}^4$  model for the ground state and first excited state of  $\text{Be}^7$ . Capture of particles from the  $S$ ,  $P$ ,  $D$ , and  $F$  partial waves by means of  $E1$ ,  $M1$ , and  $E2$  transitions is considered. The results are in excellent agreement with the experimental data presented in the preceding paper and indicate that the reaction proceeds chiefly by means of  $E1$  capture from the  $S$  and  $D$  waves. It is a surprising consequence that the  $D$  wave contributes an appreciable fraction of the total capture cross section for alpha-particle energies as low as 1 MeV. Using the same values for the reduced widths of the final states that were determined for the  $\text{He}^3(\alpha, \gamma)\text{Be}^7$  reaction, similar calculations have also yielded excellent agreement with the experimental data for both the branching ratio and the total cross section of the mirror reaction  $\text{T}(\alpha, \gamma)\text{Li}^7$ .

#### INTRODUCTION

IT has long been known that the extranuclear contributions to radiative capture reactions are appreciable,<sup>1</sup> and several such reactions have been found where these contributions play a dominant role. These reactions are necessarily nonresonant, since they do not follow from the formation of a compound state, and for this reason they have been designated as "direct-capture" reactions. Several examples of direct-capture

reactions that have been previously reported are  $\text{O}^{16}(p, \gamma)\text{F}^{17}$ ,<sup>2</sup>  $\text{Ne}^{20}(p, \gamma)\text{Na}^{21}$ ,<sup>3</sup> and  $\text{D}(p, \gamma)\text{He}^3$ .<sup>4</sup>

The reactions  $\text{He}^3(\alpha, \gamma)\text{Be}^7$  and  $\text{T}(\alpha, \gamma)\text{Li}^7$  are also of the direct-capture type. Calculations by Christy and Duck<sup>5</sup> and by Tombrello and Phillips<sup>6</sup> based on the data of Holmgren and Johnston,<sup>7</sup> have indicated that these experimental results could be understood in a

<sup>2</sup> J. B. Warren, K. A. Laurie, D. B. James, and K. L. Erdman, *Can. J. Phys.* **32**, 563 (1954).

<sup>3</sup> N. Tanner, *Phys. Rev.* **114**, 1060 (1959).

<sup>4</sup> G. M. Griffiths and J. B. Warren, *Proc. Roy. Soc. (London)* **A68**, 781 (1955).

<sup>5</sup> R. F. Christy and I. Duck, *Nucl. Phys.* **24**, 89 (1961).

<sup>6</sup> T. A. Tombrello and G. C. Phillips, *Phys. Rev.* **122**, 224 (1961).

<sup>7</sup> H. D. Holmgren and R. L. Johnston, *Phys. Rev.* **113**, 1556 (1959).

\* Supported by the U. S. Office of Naval Research.

† Present address: Physics Department, Yale University, New Haven, Connecticut.

<sup>1</sup> R. G. Thomas, *Phys. Rev.* **84**, 1061 (1951).

quantitative way. Both calculations considered extra-nuclear  $E1$  capture from the  $l=0$  partial wave of the initial state to final states that were assumed to be of the two-body form,  $A^3+\text{He}^4$ .

Recently, more accurate and extensive data have become available for both of these reactions. The  $\text{T}(\alpha, \gamma)\text{Li}^7$  reaction has been investigated by Griffiths *et al.* for alpha-particle energies between 0.5 and 1.9 MeV.<sup>8</sup> These measurements include a determination of the total cross section, the branching ratio for transitions to the ground state and first excited state, and a small amount of information concerning the angular distribution of the gamma radiation. The new  $\text{He}^3(\alpha, \gamma)\text{Be}^7$  data, which are discussed by Parker and Kavanagh in the preceding paper,<sup>9</sup> consist of the total cross section and branching ratio for alpha-particle energies between 0.4 and 5.8 MeV.

Since the form of the initial-state wave function and thus the validity of the assumption that these are direct-capture reactions depend strongly on the phase shifts for the elastic scattering, a brief summary of the work on the elastic scattering of  $\text{He}^3$  from  $\text{He}^4$  is given. The phase shifts for the reaction  $\text{He}^4(\text{He}^3, \text{He}^3)\text{He}^4$  have been determined for bombarding energies between 2.5 and 12 MeV.<sup>10-12</sup> These results indicate that:

(1) The  $S$ -wave phase shift  $\delta_0$  is accurately described by scattering from a charged hard sphere of radius  $2.8 \times 10^{-13}$  cm for alpha-particle energies below 8 MeV.

(2) The  $P$ -wave phase shifts  $\delta_1^+$  and  $\delta_1^-$  are both negative and are unequal in value. The splitting of these phase shifts shows the presence of the spin-orbit interaction that is responsible for the energy separation of the ground state and the first excited state of  $\text{Be}^7$ . The energy variation of these phase shifts is consistent with values for the reduced widths  $\theta^2$  for the two bound states that approach unity.

(3) The  $D$ -wave phase shifts  $\delta_2^+$  and  $\delta_2^-$  are approximately equal over this entire range of energies and are well represented by scattering from a charged hard sphere of radius  $2.8 \times 10^{-13}$  cm.

(4) The  $F$ -wave phase shifts  $\delta_3^+$  and  $\delta_3^-$  are positive (or zero) over this energy range, their behavior reflecting the presence of the  ${}^2F_{7/2}$  and  ${}^2F_{5/2}$  levels in  $\text{Be}^7$ .

These results indicate that the initial wave function is small over the nuclear volume for both the  $S$  and  $D$

waves and thus that the most important part of their contributions to the capture process should come from the region outside the nuclear surface. The nuclear radius of  $2.8 \times 10^{-13}$  cm determined from the energy variation of these phase shifts is in good agreement with the value of  $2.71 \times 10^{-13}$  cm for  $\text{Li}^7$  obtained from electron scattering.<sup>13</sup>

In the calculations described the following assumptions are made:

(1) The direct-capture process may be calculated using first-order perturbation theory.

(2) Only contributions to the capture matrix element from outside the nuclear surface are considered. This assumption allows the calculation to be made without considering the more difficult problem of what form the wave functions take inside the nucleus. Because of the hard-sphere character of the  $S$ - and  $D$ -wave phase shifts, this assumption is quite valid for the  $S$  and  $D$  waves which are responsible for the  $E1$  contribution to the capture process. The effect of this assumption on capture from the  $P$  and  $F$  waves is discussed with the results.

(3) The bound states of the nuclei  $\text{Li}^7$  and  $\text{Be}^7$  are described by two-body wave functions of the form  $A^3+\text{He}^4$ . The normalization of the exterior portions of these wave functions is related to their reduced widths for such a two-body configuration.

### THEORY

Considering the capture of a particle of mass  $M_1$ , charge  $Z_1$ , and magnetic moment  $\mu_1$  by a particle of mass  $M_2$ , charge  $Z_2$ , and magnetic moment  $\mu_2$ , the following expression for the differential cross section is obtained from perturbation theory:

$$\left(\frac{d\sigma}{d\Omega}\right)_{J_f} = \frac{\kappa}{2\pi\hbar V_I} \times \sum_{m_i, m_f, P=\pm 1} \frac{1}{2S+1} |\langle f, J_f m_f | H_{\text{int}}^P | i, m_i \rangle|^2,$$

where  $S$  is the channel spin,  $\kappa$  and  $P$  are the wave number and circular polarization of the radiation,  $V_I$  is the relative velocity of the two particles, and  $i$  and  $f$  refer to the initial- and final-state wave functions. In the long-wavelength approximation, considering only  $E1$ ,  $M1$ , and  $E2$  capture<sup>14</sup>:

$$H_{\text{int}}^P = \sum_M \left\{ -i \left(\frac{4\pi}{3}\right)^{1/2} P e \kappa \alpha \left(\frac{Z_1}{M_1} - \frac{Z_2}{M_2}\right) D_1^{*M, P}(\varphi_\gamma, \theta_\gamma, 0) r Y_1^{*M}(\theta, \varphi) + (-1)^M \frac{e \kappa \hbar}{2m_p c} D_1^{*M, P}(\varphi_\gamma, \theta_\gamma, 0) \right. \\ \left. \times \left[ \alpha \left(\frac{Z_1}{M_1^2} + \frac{Z_2}{M_2^2}\right) \mathbf{L} + \mu_1 \boldsymbol{\sigma}_1 + \mu_2 \boldsymbol{\sigma}_2 \right] \cdot \boldsymbol{\kappa}_1^{-M} - \left(\frac{\pi}{15}\right)^{1/2} P e \kappa^2 D_2^{*M, P}(\varphi_\gamma, \theta_\gamma, 0) \alpha^2 \left(\frac{Z_1}{M_1^2} + \frac{Z_2}{M_2^2}\right) r^2 Y_2^{*M}(\theta, \varphi) \right\}.$$

<sup>8</sup> G. M. Griffiths, R. A. Morrow, P. J. Riley, and J. B. Warren, *Can. J. Phys.* **39**, 1397 (1961).

<sup>9</sup> P. D. Parker and R. W. Kavanagh, preceding article, *Phys. Rev.* **131**, 2578 (1963).

<sup>10</sup> P. D. Miller and G. C. Phillips, *Phys. Rev.* **112**, 2048 (1958).

<sup>11</sup> C. M. Jones, A. C. L. Barnard, and G. C. Phillips, *Bull. Am. Phys. Soc.* **7**, 119 (1962).

<sup>12</sup> T. A. Tombrello and P. D. Parker, *Phys. Rev.* **130**, 1112 (1963).

<sup>13</sup> R. Hofstadter, *Rev. Mod. Phys.* **28**, 214 (1956).

<sup>14</sup> S. A. Moszkowski, in *Beta- and Gamma-Ray Spectroscopy*, edited by K. Siegbahn (North-Holland Publishing Company, Amsterdam, 1955), p. 373 ff.

The quantities  $e$  and  $m_p$  are the charge and mass of the proton;  $\alpha = M_1 M_2 / (M_1 + M_2)$ ;  $\mathbf{L}$  is the orbital angular momentum operator;  $\boldsymbol{\sigma}_i$  is the spin operator for the  $i$ th particle;  $D_\lambda^{M,P}(\varphi_\gamma, \theta_\gamma, 0)$  is an element of the rotation matrix; and  $\theta_\gamma$  and  $\varphi_\gamma$  are the polar and azimuthal angles of the gamma radiation, where the  $z$  axis is defined by the incident beam.  $\mathcal{X}_1^\mu$  is the spherical unit vector with  $z$ -axis projection  $\mu$ .

The initial wave function for the relative motion of two particles is

$$\psi_i^{M_i} = \sum_{l=0}^{\infty} [4\pi(2l+1)]^{1/2} i^l \left\{ \frac{l+1}{kr} e^{i\delta_l^+} R_l^+ + \frac{l}{2l+1} e^{i\delta_l^-} R_l^- \right\} Y_l^0(\theta, \varphi) \mathcal{X}_{1/2}^{M_i} \\ + \sum_{l=1}^{\infty} \left[ \frac{4\pi l(l+1)}{2l+1} \right]^{1/2} \frac{e^{i\alpha_l}}{kr} \{ e^{i\delta_l^+} R_l^+ - e^{i\delta_l^-} R_l^- \} Y_l^{2M_i}(\theta, \varphi) \mathcal{X}_{1/2}^{-M_i},$$

where  $k$  is the wave number,  $\mathcal{X}_{1/2}$  is the spin function for the  $\text{He}^3$  or  $\text{H}^3$ ,  $\delta_l^\pm$  is the phase shift for orbital angular momentum  $l$  and total angular momentum  $j = l \pm \frac{1}{2}$ , and the  $\alpha_l$  are related to the usual Coulomb phase shifts,  $\alpha_l = \sigma_l - \sigma_0$ .

Outside the nuclear surface the radial functions  $R_l^\pm$  can be written in terms of the regular and irregular Coulomb functions  $F_l(\eta, \rho)$  and  $G_l(\eta, \rho)$ .

$$R_l^\pm = F_l(\eta, \rho) \cos \delta_l^\pm + G_l(\eta, \rho) \sin \delta_l^\pm,$$

where  $\rho = kr$  and  $\eta = \alpha Z_1 Z_2 e^2 / \hbar^2 k$ .

The final-state wave function in this region is written

$$\psi_{f, J_f}^{m_f} = \theta_{J_f} \left[ \frac{3}{r_0 U_f^2(r_0)} \right]^{1/2} \\ \times \frac{U_f(r)}{r} \sum_{\sigma} C(1, 1/2, J_f; m_f - \sigma, \sigma) Y_1^{m_f - \sigma}(\theta, \varphi) \mathcal{X}_{1/2}^{\sigma},$$

where  $r_0$  is the nuclear radius and  $\theta_{J_f}^2 = (2\alpha r_0^2 / 3\hbar^2) \gamma_{J_f}^2$ ,  $\gamma_{J_f}^2$  being the reduced width of the bound state.  $U_f(r)$  in this external region is proportional to the Whittaker function  $W_{\eta, l}(\rho)$ . The normalization of the bound-state function used here is different from that used in Ref. 6, but is the same as that of Ref. 5.

Inserting the above wave functions into the matrix element and performing the necessary algebra one obtains, under the further assumptions that the initial mass three particle is unpolarized and that only values of  $l \leq 3$  need be considered, an expression of the following form:

$$(d\sigma/d\Omega)_{J_f} = \sigma_0(J_f) [1 + a_1(J_f) \cos\theta + a_2(J_f) \cos^2\theta \\ + a_3(J_f) \cos^3\theta + a_4(J_f) \cos^4\theta].$$

The total cross section for each transition is, thus,

$$\sigma_{\text{total}}(J_f) = 4\pi\sigma_0(J_f) [1 + \frac{1}{3}a_2(J_f) + \frac{1}{5}a_4(J_f)].$$

The coefficients  $\sigma_0$ ,  $a_1$ ,  $a_2$ ,  $a_3$ , and  $a_4$  are complicated functions of the various integrals in the matrix element. The integrations over the angle and spin variables can be done analytically leaving only the numerical evaluation of the radial integrals to be performed. These radial

integrals are of the forms

$$\int_{r_0}^{\infty} U_f(r) r^a F_l(r) dr \quad \text{and} \quad \int_{r_0}^{\infty} U_f(r) r^a G_l(r) dr,$$

where for  $l=0$  or  $2$ ,  $a=1$ , for  $l=1$ ,  $a=0$  or  $2$ , and for  $l=3$ ,  $a=2$ .

The generation of the appropriate functions, their numerical integration, and their combination to form the coefficients of the angular distribution were accomplished on the Burroughs 220 computer.

The functions  $F_l$ ,  $G_l$ , and  $U_f$  were generated by calculating two starting values of each function and then extrapolating to other values of the radial variable using the following finite-difference expression:

$$f(r-\delta)q(r-\delta) + f(r+\delta)q(r+\delta) \\ = [12 - 10q(r)]f(r) + O(\delta^6),$$

where  $f(r)$  represents the appropriate function and

$$q(r) = 1 - (\delta^2 k^2 / 12\rho^2) [-\rho^2 + 2\rho\eta + l(l+1)]$$

for the continuum functions  $F_l$  and  $G_l$ , and

$$q(r) = 1 - (\delta^2 k^2 / 12\rho^2) [\rho^2 + 2\rho\eta + l(l+1)]$$

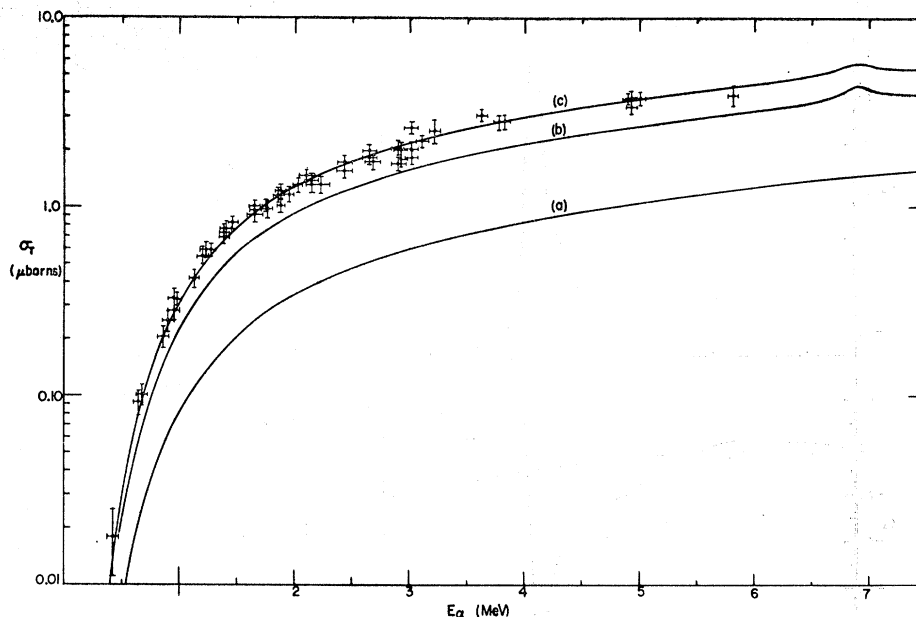
for the bound function  $U_f$ .

The starting values of the regular Coulomb function  $F_l$  were calculated at  $r_0$  and  $r_0 + \delta$  and then extrapolated to higher values of  $r$ . The functions  $G_l$  and  $U_f$  were started at large radial distances ( $\sim 80 \times 10^{-13}$  cm) and were continued inward to the nuclear radius. At the lowest energies it was necessary to go to considerably larger starting radii for  $l=2$  and  $3$  to ensure the same accuracy in  $G_l$ .

The values of  $F_l$  and  $G_l$  were checked against standard tabulations<sup>15</sup> and were found to be accurate to better than 0.5% at each point. The values of  $U_f$  were checked against values of the Whittaker function obtained from its integral form; they were found to agree to better

<sup>15</sup> Arnold Tubis, Los Alamos Scientific Laboratory Report LA-2150, 1957 (unpublished); I. Bloch, M. H. Hull, A. A. Broyles, W. G. Bouricius, B. E. Freeman, and G. Breit, Rev. Mod. Phys. 23, 147 (1951).

FIG. 1. The total cross section in microbarns for the  $\text{He}^3(\alpha, \gamma)\text{Be}^7$  reaction. The experimental points are from Ref. 9 and correspond to the sum of the two transitions. The theoretical curves are: (a) the cross section for transitions to the first excited state, (b) the cross section for transitions to the ground state, and (c) the sum of curves (a) and (b).



than 0.2%. The expressions used for starting values of the functions are summarized in the Appendix.

These functions were multiplied together and integrated numerically using the trapezoidal rule to give the radial integrals. A value of  $\delta = 10^{-14}$  cm was found to be adequate, and the integrals had usually converged at values of  $r < 5 \times 10^{-12}$  cm.

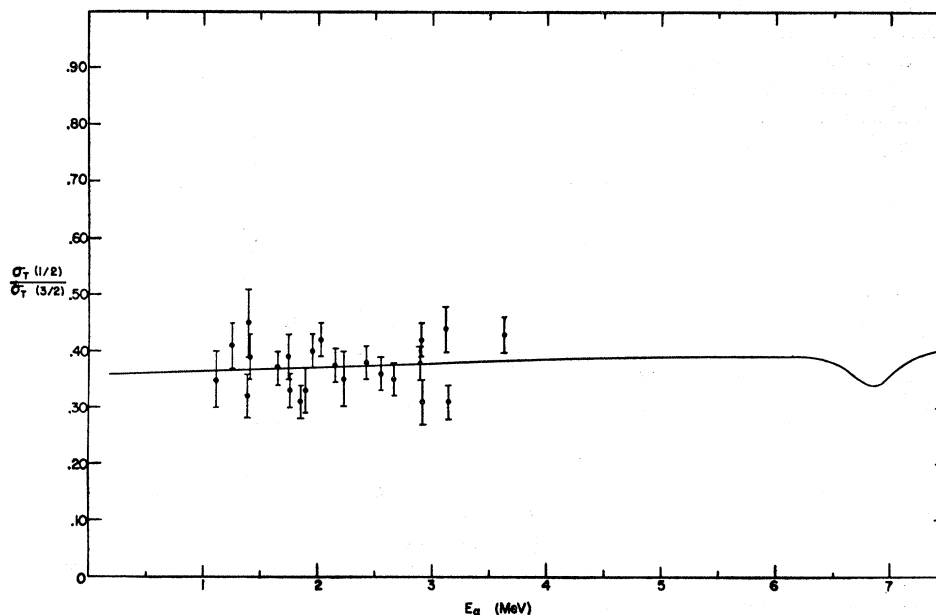
The values of the phase shifts used in these calculations were obtained from the scattering experiments discussed in the preceding section.

(1) The  $S$ - and  $D$ -wave phase shifts were assumed equal to the hard-sphere phase shifts corresponding to

a nuclear radius of  $2.8 \times 10^{-13}$  cm. Since this assumption is valid for the energies covered by the  $\text{He}^4(\text{He}^3, \text{He}^3)\text{He}^4$  data, we have considerable confidence in its validity at lower energies. The  $S$ - and  $D$ -wave phase shifts for the  $\text{He}^4(t, t)\text{He}^4$  reaction were also assumed to have this form.

(2) The  $P$ -wave phase shifts  $\delta_1^+$  and  $\delta_1^-$  for  $E_\alpha \geq 3.0$  MeV were taken from smooth curves drawn through the phase shifts derived from the  $\text{He}^4(\text{He}^3, \text{He}^3)\text{He}^4$  scattering data. At lower energies they were obtained by normalizing multiples of the  $P$ -wave hard-sphere phase shift to the derived values at  $E_\alpha = 3$  MeV. The

FIG. 2. The ratio of the cross section for transitions to the first excited state to the cross section for transitions to the ground state for the  $\text{He}^3(\alpha, \gamma)\text{Be}^7$  reaction. The experimental points were taken from Ref. 9.



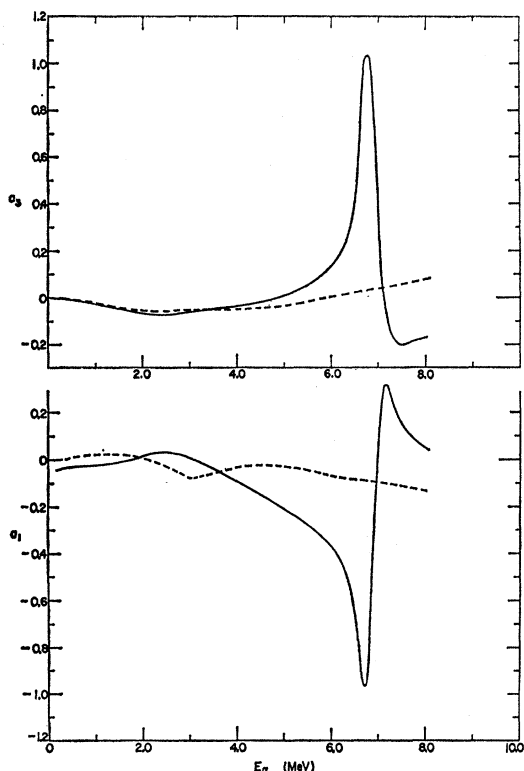


FIG. 3. The predicted angular distribution coefficients  $a_1$  and  $a_3$  for the  $\text{He}^3(\alpha, \gamma)\text{Be}^7$  reaction. The solid curves are for the ground-state transition; the broken curves are for the first excited state transition.

capture from the  $P$  waves was not calculated for  $\text{T}(\alpha, \gamma)\text{Li}^7$ , because no values of the  $P$ -wave phase shifts were available.

(3) The  $F$ -wave phase shifts  $\delta_3^+$  and  $\delta_3^-$  were taken from smooth curves drawn through those values derived from the  $\text{He}^4(\text{He}^3, \text{He}^3)\text{He}^4$  data. These phase shifts were assumed to be identically zero below  $E_\alpha = 3.5$  MeV. Capture from the  $F$  waves was not calculated for the  $\text{T}(\alpha, \gamma)\text{Li}^7$  reaction because values of these phase shifts were not available.

## RESULTS

### $\text{He}^3(\alpha, \gamma)\text{Be}^7$

Two remaining parameters  $\theta_{3/2}^2$  and  $\theta_{1/2}^2$  are still free and may be obtained by comparison of the calculated values for  $\sigma_{\text{total}}$  and  $\sigma(1/2)/\sigma(3/2)$  to the experimental data. The reduced widths are, however, independent of the bombarding energy and, therefore, can only affect the normalization of the theoretical curves, not their shape. Using the experimental values for the total cross section shown in Fig. 1 and the branching ratio given in Fig. 2, these parameters are found to be  $\theta_{3/2}^2 = 1.25$  and  $\theta_{1/2}^2 = 1.05$  and are thus seen to be close to the values of approximately unity expected as a result of the analysis of the  $P$ -wave phase shifts.<sup>10</sup> If the value of the

TABLE I. The values of  $\theta_{3/2}^2$  and  $\theta_{1/2}^2$  for the bound states of  $\text{Be}^7$  obtained for several values of the nuclear radius. (This variation of  $r_0$  occurs only in the evaluation of the radial integrals and does not affect the values of the phase shifts.)

$r_0$ (cm)	$\theta_{3/2}^2$	$\theta_{1/2}^2$
$2.4 \times 10^{-13}$	1.86	1.55
$2.8 \times 10^{-13}$	1.25	1.05
$3.2 \times 10^{-13}$	0.88	0.73

nuclear radius used in the evaluation of the radial integrals is changed, then a corresponding variation of  $\theta_j^2$  results, but the over-all agreement of the calculated and experimental curves is not affected. The variation of  $\theta_j^2$  with  $r_0$  is shown in Table I.

As is indicated by Figs. 1 and 2, the agreement is excellent over the entire energy range. Figures 3 and 4 show the angular distribution coefficients calculated on the basis of this model. The large variations in these coefficients near  $E_\alpha = 7$  MeV clearly show the predicted effects of the  ${}^2F_{7/2}$  level of  $\text{Be}^7$ . The calculated effect of this resonance on the total cross section is almost negligible, however. Figure 5 gives the fractional contribution to the total cross section for each transition: (a)  $E1$  capture from the  $l=0$  partial wave, (b)  $E1$

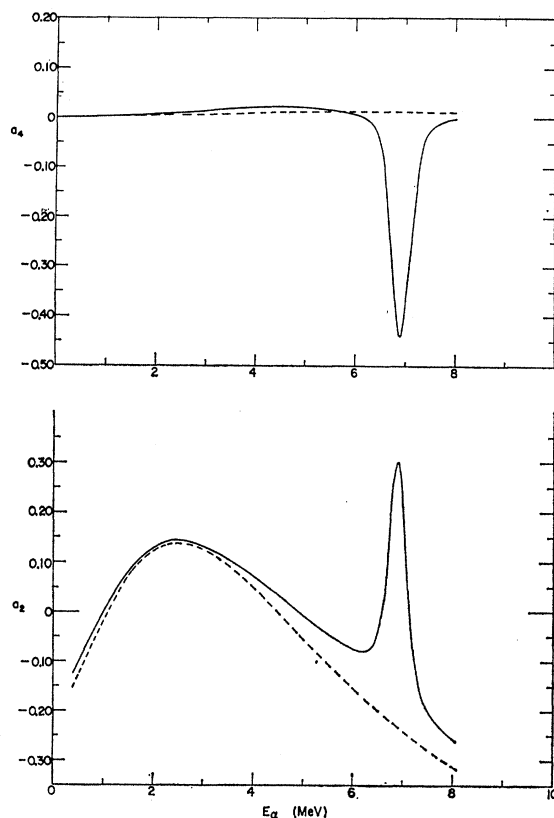
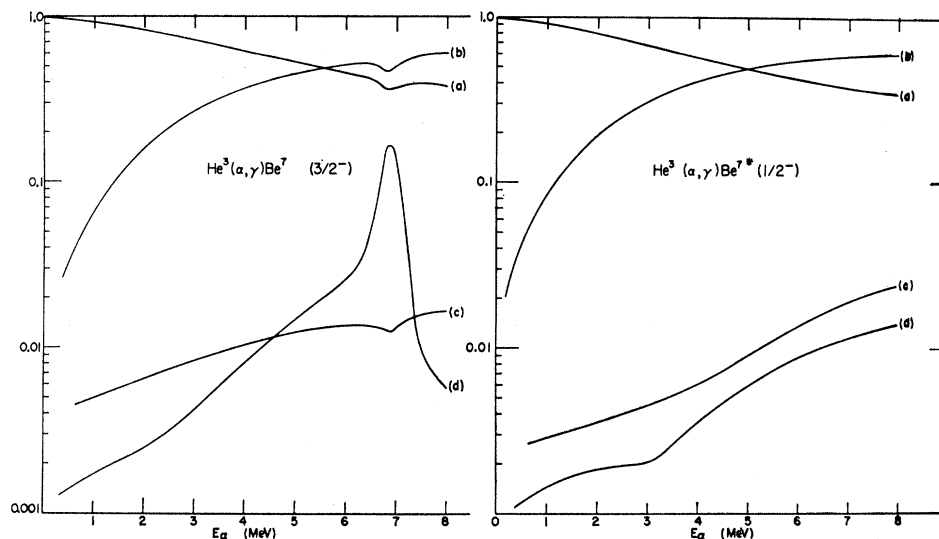


FIG. 4. The predicted angular distribution coefficients  $a_2$  and  $a_4$  for the  $\text{He}^3(\alpha, \gamma)\text{Be}^7$  reaction. The curves have the same significance as those of Fig. 3.

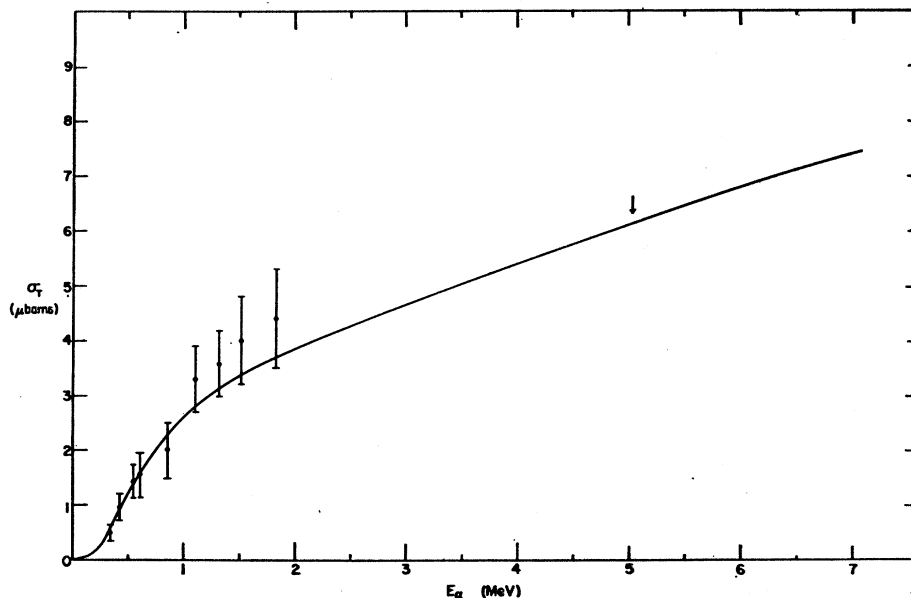
FIG. 5. The fraction of the total cross section for the  $\text{He}^3(\alpha, \gamma)\text{Be}^7$  reaction contributed by (a)  $E1$  capture from the  $l=0$  partial wave, (b)  $E1$  capture from the  $l=2$  partial wave, (c)  $M1$  capture from the  $l=1$  partial wave, and (d)  $E2$  capture from the  $l=1$  and  $l=3$  partial waves.



capture from the  $l=2$  partial wave, (c)  $M1$  capture from the  $l=1$  partial wave, and (d)  $E2$  capture from the  $l=1$  and  $l=3$  partial waves. Except for a small region near the resonance, the combined contributions from the  $M1$  and  $E2$  capture are below 4% of the total cross section, and below  $E_\alpha=3$  MeV they contribute less than 1%. Therefore, since the  $\text{He}^3(\alpha, \gamma)\text{Be}^7$  data have a total uncertainty of approximately 10% we would have obtained equally good fits to the total cross section and the branching ratio if we had neglected the  $M1$  and  $E2$  contributions completely. The relatively small size of the external  $M1$  and  $E2$  contributions calculated above also gives us some confidence in our assumption neglecting the internal contributions of these multipoles

even though the pertinent scattering phase shifts are not of the hard-sphere form. Indeed, it should be emphasized here that the good agreement which we were able to get between the calculations and the observed cross section and branching ratio is due to the rather fortunate circumstance that over the entire energy range of this experiment the reaction proceeds almost completely through the partial waves which can be described by hard-sphere phase shifts, rescuing us from our neglect of the region inside the nuclear radius. Near the  ${}^2F_{7/2}$  level in  $\text{Be}^7$  this happy situation will no longer exist, but in the absence of experimental data in this region no determination of the ratio of nuclear to extranuclear capture is possible. For this reason the large

FIG. 6. The total cross section in microbarns for the  $\text{T}(\alpha, \gamma)\text{Li}^7$  reaction. The data are from Ref. 8; the solid curve is the theoretical prediction based on the reduced widths  $\theta_{3/2}^2$  and  $\theta_{1/2}^2$  determined from the  $\text{He}^3(\alpha, \gamma)\text{Be}^7$  reaction. The arrow indicates the position of the  ${}^2F_{7/2}$  state of  $\text{Li}^7$ .



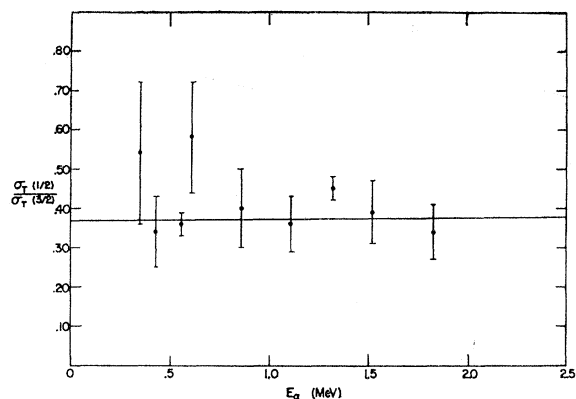


FIG. 7. The ratio of the cross section for the first excited state transition to the cross section for the ground-state transition in the  $T(\alpha, \gamma)Li^7$  reaction. The data are from Ref. 8; the solid line has the same significance as in Fig. 6.

variations in the angular distribution coefficients near the resonance must be considered only as an indication of their possible behavior.

It is important to note that the data cannot be fitted at energies above  $E_{\alpha}=1.0$  MeV unless the  $E1$  capture contributed by the  $D$  waves is considered.

### $T(\alpha, \gamma)Li^7$

The values of  $\theta_j^2$  for  $Li^7$  were assumed to have been determined from the analysis of the  $He^3(\alpha, \gamma)Be^7$  data and were fixed at  $\theta_{3/2}^2=1.25$  and  $\theta_{1/2}^2=1.05$ . The resulting fits to the total cross section and the branching ratio for the  $T(\alpha, \gamma)Li^7$  reaction are shown in Figs. 6 and 7. As these curves show, the theory and the data agree very well, even when no parameters remain to be adjusted.

For this calculation only  $E1$  capture from the  $S$  and  $D$  waves was considered. This assumption was felt to be justified by the small contributions to the total cross section from  $M1$  and  $E2$  capture in the  $He^3(\alpha, \gamma)Be^7$  reaction. This justification is welcome in view of the absence of values for the  $P$ - and  $F$ -wave phase shifts. Because of the neglect of  $F$ -wave capture, no effects due to the  ${}^2F_{7/2}$  state in  $Li^7$  are predicted in the curves in Figs. 6 and 8.

With this limitation only the coefficients  $\sigma_0$  and  $a_2$  are nonzero. The value of  $a_2$  is shown in Fig. 8. Using these restricted results the theory can be compared to

TABLE II. Comparison of the theoretical and experimental angular distributions for the  $T(\alpha, \gamma)Li^7$  reaction. The data quoted are those of Ref. 8. The theoretical calculations include only the coefficient  $a_2$ .

$\bar{E}_{\alpha}$ (MeV)	Intensity ratio	Measured	Calculated
0.56	$0^{\circ}/90^{\circ}$	$1.05 \pm 0.06$	1.12
1.32	$0^{\circ}/90^{\circ}$	$1.28 \pm 0.04$	1.32
	$45^{\circ}/90^{\circ}$	$1.06 \pm 0.06$	1.16
	$135^{\circ}/90^{\circ}$	$1.02 \pm 0.06$	1.16

the angular distributions obtained by Griffiths *et al.*<sup>8</sup> This comparison is given in Table II. The agreement is reasonable but is not correct in detail. This lack of complete agreement may only reflect the absence of  $a_1$  and  $a_3$  that would have come from the  $P$ - and  $F$ -wave capture. Though these terms do not contribute to the total cross section, they can exert significant influence on the angular distribution.

### CONCLUSIONS

The excellent agreement between theory and experiment for these two reactions indicates the success of this direct-capture model. On the basis of this successful model we are then able to make reliable extrapolations of the cross section and branching ratio into experimentally inaccessible regions, e.g., extrapolation of the cross section to thermal energies for use in astrophysical calculations.<sup>9</sup> In addition, the fit of the theory to the data provides us with information about properties, such as the reduced width, of the various bound states of the final nucleus.

However, due to certain deficiencies in the experimental data, we have not been able to make a complete examination of the theory. A list of possible measurements that should allow a more detailed test of the model includes

(1) A determination of the phase shifts for  $T(\alpha, \alpha)T$  scattering, eliminating the present dependence on the properties of the mirror reaction  $He^3(\alpha, \alpha)He^3$ , would permit a more valid comparison of the theory with the present  $T(\alpha, \gamma)Li^7$  measurements and would permit a more complete calculation of the angular distributions for the  $T(\alpha, \gamma)Li^7$  reaction.

(2) Angular distributions for the  $He^3(\alpha, \gamma)Be^7$  reaction should be measured for comparison with the calculations given here. However, these measurements are difficult to perform because of the small cross sections involved.<sup>9</sup>

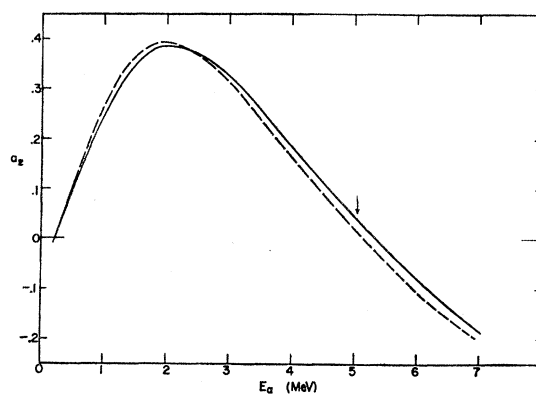


FIG. 8. The predicted angular distribution coefficient  $a_2$  for the  $T(\alpha, \gamma)Li^7$  reaction. The solid curve is for the ground-state transition; the broken curve is for the first excited-state transition. The calculated values of  $a_1$ ,  $a_3$ , and  $a_4$  are identically zero because capture from the  $P$  and  $F$  waves was neglected for this reaction. The arrow indicates the position of the  ${}^2F_{7/2}$  state of  $Li^7$ .

(3) Measurements of the differential capture cross section near the  ${}^2F_{7/2}$  resonance should allow a determination of the relative importance of the nuclear and the extranuclear contributions to the matrix element for  $E2$  capture.

#### ACKNOWLEDGMENTS

We would like to acknowledge helpful conversations with Professor G. M. Griffiths, whose experimental data

provided the original incentive for this work. We are also grateful to Dr. A. C. L. Barnard for making available the values of the low energy  $\text{He}^3 + \alpha$  phase shifts prior to their publication. To Barbara Zimmerman go our special thanks for her help in programming the subroutines for the Coulomb and bound-state functions. In this regard, thanks are also due to Dr. John Domingo for his help in checking the accuracy of the various functions generated.

#### APPENDIX

The expression used for calculating starting values of the bound-state wave function  $U_l$  at large radial distances is

$$U_l(\rho, \eta, l) = \left\{ \frac{\rho}{[\rho^2 + 2\rho\eta + l(l+1)]^{1/2}} \right\}^{1/2} \{[\rho^2 + 2\rho\eta + l(l+1)]^{1/2} + \rho + \eta\}^{-\eta} \\ \times \left[ \frac{1}{\rho} \{[\rho^2 + 2\rho\eta + l(l+1)]^{1/2} + [l(l+1)]^{1/2}\} + \frac{\eta}{[l(l+1)]^{1/2}} \right]^{[l(l+1)]^{1/2}} \exp\{-[\rho^2 + 2\rho\eta + l(l+1)]^{1/2}\}.$$

This form is obtained directly using the JWKB approximation.<sup>16</sup>

The starting values of the irregular Coulomb function  $G_l$  were calculated using a modified form of the JWKB wave function.<sup>9</sup>

$$G_l(\eta, \rho) = \{\rho / [\rho^2 - 2\rho\eta - l(l+1)]^{1/2}\}^{1/2} \sin(\varphi_l + \sigma_l + \frac{1}{2}\pi - \frac{1}{2}l\pi),$$

where  $\sigma_l$  is the Coulomb phase shift for the  $l$ th partial wave, and

$$\varphi_l = \eta + [\rho^2 - 2\rho\eta - l(l+1)]^{1/2} - \eta \ln\{\rho - \eta + [\rho^2 - 2\rho\eta - l(l+1)]^{1/2}\} \\ - [l(l+1)]^{1/2} \tan^{-1} \left\{ \frac{[l(l+1)]^{1/2} [\rho^2 - 2\rho\eta - l(l+1)]^{1/2}}{\rho\eta + l(l+1)} \right\} + [l(l+1)]^{1/2} \tan^{-1}\{[l(l+1)]^{1/2}/\eta\}.$$

Starting values of the regular Coulomb function  $F_l$  were obtained near the nuclear radius using its exact power series expansion.<sup>15</sup>

$$F_l(\eta, \rho) = \frac{2^l}{(2l+1)!} \left[ \frac{1 \times (1+\eta^2) \times (4+\eta^2) \times \cdots \times (l^2+\eta^2) 2\pi\eta^{-1}}{e^{2\pi\eta} - 1} \right]^{1/2} \sum_{n=l+1}^{\infty} A_n^l(\eta) \rho^n,$$

where  $A_{l+1}^l = 1$ ,  $A_{l+2}^l = \eta/(l+1)$ , and

$$(n+l)(n-l-1)A_n^l = 2\eta A_{n-1}^l - A_{n-2}^l.$$

These expressions for the starting values, in conjunction with the finite-difference continuation method discussed in the text, have been found to give good accuracy over the entire range covered by these calculations.

<sup>16</sup>L. I. Schiff, *Quantum Mechanics* (McGraw-Hill Book Company, Inc., New York, 1955), p. 184.